Short-term Biodistribution and Clearance of Intravenously Administered Silica Nanoparticles

Nadia Waegeneers[a,*], Anne Brasseur[a], Elke Van Doren[b], Sara Van der Heyden[c], Pieter-Jan Serreyn[c], Luc Pussemier[a], Jan Mast[b], Yves-Jacques Schneider[d], Ann Ruttens[a], Stefan Roels[c]

[a]Trace Element Service, Veterinary and Agrochemical Research Centre (CODA-CERVA), Leuvensesteenweg 17, B-3080 Tervuren, Belgium

[b]Electron Microscopy Service, Veterinary and Agrochemical Research Centre (CODA-CERVA), Groeselenberg 99, B-1180 Uccle, Belgium

[c]Scientific Service of Orientation and Veterinary Support, Veterinary and Agrochemical Research Centre (CODA-CERVA), Groeselenberg 99, B-1180 Uccle, Belgium

[d]Laboratory of Cellular, Nutritional and Toxicological Biochemistry, Institute of Life Sciences, Université Catholique de Louvain, 5 Croix du Sud, B-1348 Louvain-la-Neuve, Belgium

*Corresponding author: nadia.waegeneers@sciensano.be

ABSTRACT

Recently, concerns have been raised about potential adverse effects of synthetic amorphous silica, commonly used as food additive (E551), since silica nanoparticles have been detected in food containing E551. We examined the biodistribution and excretion in female Sprague-Dawley rats of NM-200, a well characterized nanostructured silica representative for food applications. A single intravenous injection of NM-200 was applied at a dose of 20 mg/kg_{bw}, followed by autopsy after 6 and 24 hours. The main organs where silicon accumulated were liver and spleen. The silicon concentration significantly decreased in spleen between 6 and 24 hours. In liver the tendency was the same but the effect was not significant. This could be due to clearance of the spleen to the liver via the splenic vein, while liver clearance takes more time due to hepatic processing and biliary excretion. In treated animals the liver showed in addition a prominent increase of macrophages between both evaluation moments. Within the first 24 hours, silicon was mainly excreted through urine. Further studies are necessary to evaluate the

toxicokinetics of different types of silica nanomaterials at lower exposure doses in order to be able to predict kinetics and toxicity of silica nanoparticles depending on their physicochemical characteristics.

Keywords: Nano; Synthetic amorphous silica; In vivo; Distribution; Intravenous exposure

1. INTRODUCTION

Silicon dioxide, briefly referred to as silica, is widely used in the food industry. In Europe, synthetic amorphous silica is an approved food additive (E551), used as anticaking agent or as carrier for emulsifiers and colors [1]. Part of this silica may be in nanoparticle form [2, 3] and some types of nanosilica have shown liver toxicity in animal studies after a long-term oral exposure to high doses [4, 5]. It is currently still unknown whether this toxicity is due to the silica nanoparticles present, to (partially) dissolved silica or to a combination of both [2,5], as the oral absorption and biokinetics of food-grade nanosilica have not been well explored. Lee et al. [6] demonstrated a gastrointestinal absorption <4% after a single oral dose administration of 500 mg/kg food-grade nanosilica, while other studies report absorption levels below 0.25% [7, and references therein]. It seems that gastrointestinal absorption of nanosilica decreases with increasing treatment dose, possibly due to intestinal gelation of silica [5], although changes in particle stability, aggregation and surface properties following interaction with luminal factors present in the gastrointestinal tract may influence the bioavailability of nanosilica as well [8]. Lee et al. [6] demonstrated that the oral absorption of silica nanoparticles highly depends on the presence of sugar or proteins, presumably due to their surface interaction on nanoparticles, while Sakai-Kato et al. [9] found differences in nanosilica agglomeration depending on fed/fasting conditions. All these factors complicate the comparison of different studies on biodistribution and toxicokinetics of food-grade nanosilica after oral ingestion.

Upon intravenous (IV) administration, gastrointestinal interactions and absorption are by-passed and besides toxicity, other aspects of toxicokinetic processes, such as tissue distribution and elimination, can be studied in detail. Single dose IV studies noted no or low reversible histological or tissue effects of silica nanoparticles in mice [10, 11], while long-term repeated dose IV studies showed significant tissue injury or potential dysfunction of biliary excretion and glomular filtration in mice [12, 13]. Three consecutive IV injections of the silica nanomaterial NM-203 in rats induced hepatotoxicity, thrombocytopenia and even animal death at the highest dose of 3 x 20 mg/kg [14], but no DNA damage was induced in liver, spleen or lung.

After IV treatment of mice, nanosilica mainly accumulates in liver and spleen, but some accumulation is also reported in lung or in kidney [10-12, 15-17]. Zhuravskii et al. [17] reported the retention of amorphous nanosilica in rat liver up to 60 days after IV injection, causing liver tissue remodeling and development of fibrosis. The observed nanosilica concentrations in liver 24h after IV injection are in general higher than or equal to the nanosilica concentrations in spleen for rats and mice ([18-20], but a study in which mice tissue concentrations were measured at different moments within the first 24h suggests that silica is already rapidly cleared from both organs within this timeframe and that nanosilica concentrations might initially be higher in spleen [19]. Quantitative information about the tissue distribution within the first 24 hours after IV treatment is, however, still scarce, especially for food-grade nanosilica.

Silica nanoparticles have been shown to be actively excreted by mice within a few days after IV administration, mainly by the urinary tract but also within feces, due to particle excretion through the biliary route [19]. Nevertheless, part of the silica nanoparticles can reside relatively long in the body: in some studies, particles were still detected in the liver and spleen up to 8 weeks after injection [16, 19, 21]. The biodistribution and the excretion rate of nanosilica after IV administration is not uniform among

different animal studies and may be affected by the particle size [10, 15, 21-22], the particle shape [12, 22-23], the presence (and type) of a coating [10-12, 22] and the gender of the animal [18].

The majority of the nanosilica toxicokinetic studies are performed in the context of biomedical applications and have not used food-grade nanosilica, which may have different kinetics than e.g. mesoporous nanosilica [22]. The purpose of the present study was therefore to examine the short-term (≤ 24h) toxicokinetics after IV administration of a well characterized food-grade silica nanomaterial, NM-200, selected in the OECD (Organization for Economic Co-operation and Development) testing program [24], as quantitative information about the tissue distribution within the first 24 hours is still scarce. NM-200 has already been studied in the NANOGENOTOX project where a single dose of NM-200 (precipitated silica) or NM-203 (fumed silica) was administered intravenously to male and female rats. Biodistribution and excretion of silicon (Si) was recorded after 24 hours up to day 90 [18]. The toxicokinetics within the first 24h after a single dose of NM-200 were, however, not yet studied. To be complementary to the NANOGENOTOX study, the same animal model (rat) and an identical treatment dose of 20 mg/kg_{bw} was applied.

2. METHODS

2.1. Preparation of nanomaterial dispersions used for IV injections

NM-200, a representative test material of uncoated precipitated synthetic amorphous silica (SAS) was obtained from the Joint Research Centre Repository (JRC, Ispra, Italy). This material was produced by precipitation. NM-200 has been well characterized previously in the OECD testing program [25]. NM-200 was dispersed in phosphate buffered saline (PBS; Sigma-Aldrich) to mimic the pH, ionic strength and

osmolarity of body fluids and dispersed using the generic NANOGENOTOX dispersion protocol [26] as described in [3]. The silica concentration in the dispersion used for IV injection was 8 mg SiO_2/mL. All suspensions were prepared freshly just prior to use. PBS was used as vehicle control.

2.2 Nanoparticle Dispersion Characterization

The morphological characteristics of the dispersed NM-200 in PBS were analyzed qualitatively and quantitatively by transmission electron microscopy (TEM) as described in [3].

The hydrodynamic diameter of the dispersed NM-200 particles was analyzed by particle tracking analysis (PTA) as described in [27].

2.3. In Vivo Experimental Design

Nine-week-old female specific pathogen free Sprague-Dawley rats were purchased from Harlan (Horst, The Netherlands). The animals were allowed to acclimatize for one week and at the start of the experiment they were individually housed in metabolic cages at room temperature (21 ± 2°C) with a relative humidity of 50 ± 20% and a 12 h light/dark reversed cycle. The body weight of the animals at the beginning of the study was 220 ± 13 g. Water and standard food (RMH-B, AbDiets, The Nederland) were given *ad libitum*, except for the 12-hour period prior to the IV injections where they were deprived from food. The study was designed according to the European and national guidelines for the care and use of laboratory animals as well as the OECD guidelines for chemicals [28] and the study protocol was approved by the joint animal welfare committee of the Veterinary and Agrochemical Research Centre (CODA-CERVA) and the Scientific Institute of Public Health (ISP-WIV) prior to the onset of the study.

At the start of the trial rats were randomly divided into four groups of five animals. Two groups received 519 ± 58 µl (equaling a dose of 20 mg/kg bw) of NM-200 suspended in PBS while the two control groups received 546 ± 42 µl of PBS. The administered volumes were adapted to the weight of the animals. The intravenous injection was given in the tail vein while animals were under anesthesia using isoflurane. One group of each was necropsied after 6 hours and the remaining two groups after 24 hours.

At each time interval the selected animals were euthanized by intramuscular injection of ketamine-medetomidine, followed by exsanguination via the jugular vein. Blood was collected in a tube coated with K_2EDTA preventing blood clotting (BD vacutainer EDTA, Becton Dickinson) for silicon measurements. Following tissues were sampled at autopsy: liver, kidney, pancreas, spleen, brain, heart, lungs, leg muscle, uterus, ovaries, bladder, small intestine, colon, stomach and the contents of stomach and intestines, as well as urine and feces produced during the experiment. The walls of the stomach and intestines were washed twice with PBS to remove the remaining content. A subsample of the organs was fixed in formaldehyde for histopathology while the rest was frozen at -20°C for silicon analysis.

2.4. Histological and immunohistochemical analysis

For histopathology, attention was paid to sample for each type of organ similar parts in all rats. The samples were fixed in a 4 % phosphate-buffered formaldehyde solution (Sigma-Aldrich, 40% solution diluted 10 times), processed routinely, paraffin-embedded, and sectioned at 5-µm thickness by a microtome. Sections were then stained with haematoxylin-eosin staining. The samples were light microscopically (Olympus BX50) assessed. For the immunohistochemical staining of macrophages, the monoclonal antibody CD68 (MCA341R; AbD Serotec, Biorad, France) was applied on paraffin sections of liver, spleen and lungs at a dilution of 1:100. For visualization Envision/HRP mouse (DAB+) kit (K4007; DAKO, Glostrup, Denmark) was used for immunolabeling. This kit also blocks endogenous peroxidase. To

demask the epitope we used citrate buffer pH 6 (S2369; DAKO, Glostrup, Denmark) in a pressure cooker. The slides were evaluated qualitatively and quantitatively by the pathologist (e.g. number and concentration of microgranulomas).

2.5. Silicon Analyses

Organ samples were thawed prior to their preparation for silicon analysis. Organs and tissue samples with a mass greater than 0.55 g, were homogenized (Silent Crusher M – Heidolph) and divided in subsamples prior to mineralization, while smaller organs were mineralized entirely. Between 0.009 and 0.74 g of each sample was added to a 50 ml polypropylene *Digi*TUBE (SCP Science, France), followed by the addition of 0.563 to 2.25 ml of a nitric acid 68% - hydrofluoric acid 48% mixture (8:1 v:v). The volume of the acid mixture depended on the available mass of tissue to ensure relatively uniform dilution factors and limits of quantification. For each tissue type, approximately the same amount of mass was mineralized. Samples were predigested for 14 h at room temperature, followed by a 7 h-mineralisation at 90°C in a DigiPREP MS Digestion system (SCP SCIENCE, France) at room pressure. Whole blood was used for total silicon measurements. After cooling, the digests were further diluted with MilliQ water or 2% acid solution (HNO_3-HF, 8:1, v:v), depending on the tissue mass, to reach a total acid concentration of 4-5%. The use of glass equipment was avoided during sample preparation to prevent Si contamination.

Samples were measured using the Agilent 8800 triple quadrupole ICP-MS (Agilent, Belgium), equipped with a non-quartz sample introduction system consisting of a perfluoroalkyl (PFA) Microflow nebulizer, a 2.5 mm ID sapphire injector and a PFA spray chamber. Silicon was measured at m/z 28 in MS/MS mode. Hydrogen was used as reaction gas because preliminary experiments with the reference material BCR-185r (Bovine liver, JRC, Belgium; not certified for Si; used as such or spiked with Si at 100 mg/kg) revealed that interferences were largely eliminated compared to results obtained without gas or with

helium as collision gas. The resulting silicon concentrations were expressed in mg Si/kg fresh weight. To each mineralization batch quality control measures were added, including four procedure blanks, five samples of BCR-185r (Bovine liver, JRC, Belgium) and a Si standard solution every 20 samples to monitor instrument drift.. Additionally four samples of BCR-185r spiked with Si at 100 mg/kg were added to each batch. If instrument drift was above 15%, (part of) the batch was reanalysed.

The limit of detection (LOD) was calculated based on 25 procedure blanks (digested acid mixture) and confirmed by 15 independent digestions of a reference sample containing a low amount of silicon (BCR-185r; bovine liver). The standard deviation (*s*) was calculated for both measurement series. LOD in the measurement solution was calculated as 3*s*. This value was transformed in tissue concentrations by multiplying it with the applied dilution factor, and corresponds to LOD values in the matrix ranging from 5 to 14 mg/kg (see paragraph 3.3 of the results section)

2.6. Statistical Analysis

Results were statistically analyzed using UNISTAT 6.0 for Excel (UNISTAT Ltd., USA). Outliers were identified by the Grubb's test and excluded from the calculation of the mean and the standard deviation. Differences between treatments were analyzed using a one-way ANOVA and the Tukey HSD multiple comparison test. The level of significance in the statistical analysis was $\alpha = 0.05$.

3. RESULTS

3.1. Characterization of the NM-200 dispersions

Regarding particle characterization, NM-200 was characterized by two different techniques, TEM and PTA, as suggested by the OECD [24]. The dispersed agglomerates/aggregates had a fractal-like

morphology while primary particles of the NM were mainly round or ellipsoid, suggesting a spherical to ellipsoidal 3D structure (Fig. 1). The number-based distribution of the minimal external size of the aggregates/agglomerates in the dispersion, as measured by TEM, had a median Feret-min value of 37 nm and ranged from 5 to 695 nm (Fig. 2). The diameter, which ranged from 7 to 778 nm, was 53 nm in median. The size distribution of particles was not normally distributed.

The mean hydrodynamic diameter of the dispersed NM-200 measured by PTA was 171 ± 7 nm, which is significantly larger than the TEM results. Since the limit of detection of the NanoSight device used for PTA analysis is 50 nm, measurements were biased because primary particles and small aggregates/ agglomerates remained undetected.

Visual evaluation of the dispersions showed that they were stable for at least 30 min, with a beginning of visual deposit after 2h, which disappeared after a few minutes of vortexing.

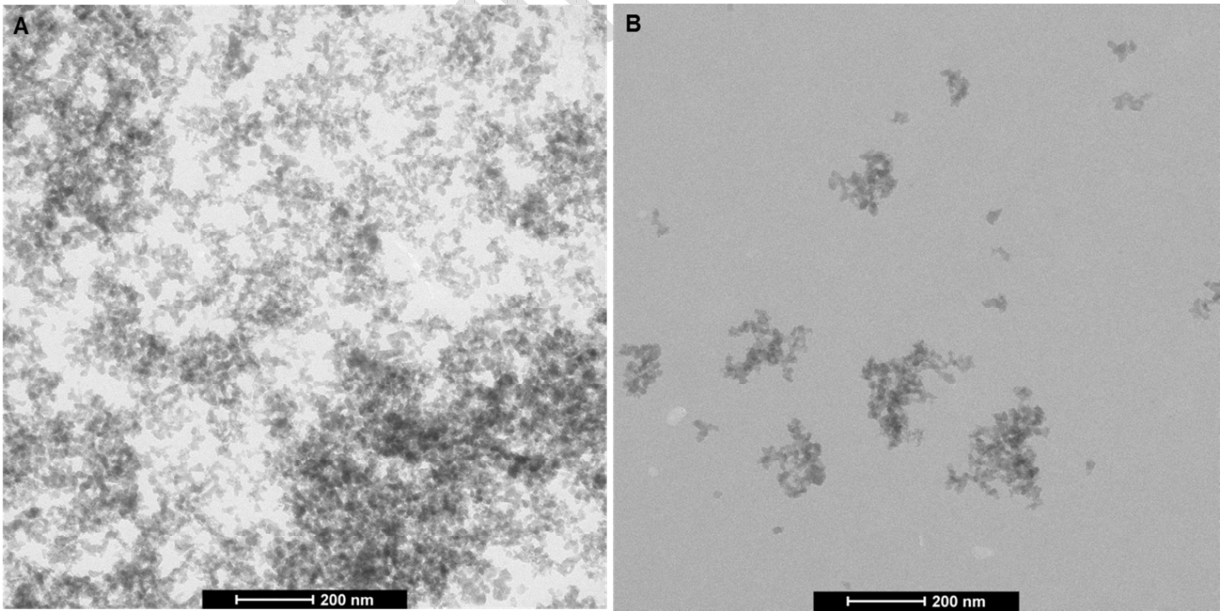

Fig. 1. Representative TEM images of the NM-200 dispersion (A) undiluted, prepared for in vivo use as such, and (B) diluted 100 times in PBS for quantitative TEM characterization.

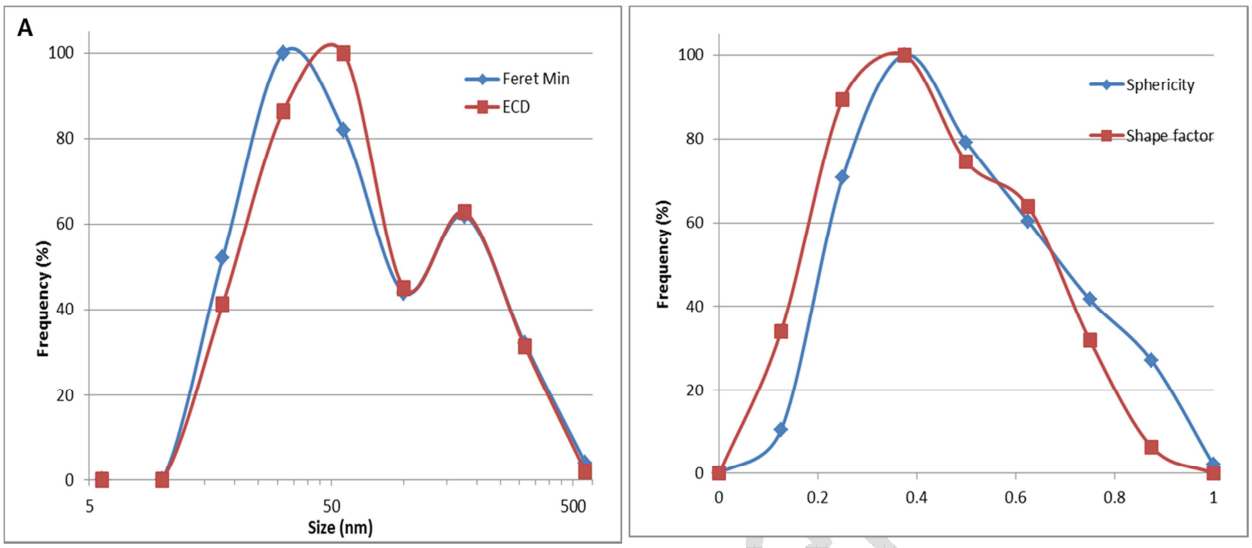

Fig. 2. Summary of the quantitative TEM characterization of silica NM-200 dispersed for in vivo use: (A) Feret-Min and ECD (equivalent circle diameter), and (B) sphericity and shape factor.

3.2. Histological and immunohistochemical analysis

No histopathological changes were detected in the organs of rats of the 6h-group, neither in the animals treated with silica, nor within the control group. In the 24h-group, both treated and control rats showed mild interstitial pneumonia. This could, however, be due to secondary conditions or infections, unrelated to the silica administration [29]. Furthermore, no abnormalities were detected on Haematoxylin-eosin staining for both groups.

The immunohistochemical strain for macrophages (CD68) revealed no clear changes in tissues of spleen and lungs, both for control and silica treated animals. However, in treated animals the liver clearly showed a prominent increase of macrophages in time: microgranulomas increased in number and concentration between 6h and 24h after injection of silica.

3.3. Silicon tissue distribution

The LOD for silicon in the measurement solution was 5.2 µg/l when based on procedural blank solutions. When based on digested BCR-185r samples, the LOD was 5 mg/kg in the matrix, corresponding to 20 µg/l in the measurement solution. As the latter limit includes matrix effects, this one was applied to the rat tissues. The LOD values in animal tissues ranged from 5 mg/kg (in e.g. liver, kidney and blood) to 14 mg/kg (in bladder). The average silicon concentration measured in BCR-185r was 4.1 ± 2.6 mg/kg (N = 53), which, although below the LOD, agreed on average well with the value of 5 ± 0.6 mg/kg measured by Klemens and Heumann [5].The average silicon concentration measured in spiked BCR-185r was 119 ± 17 mg/kg (N = 63), which was close to the expected value of 105 mg/kg.

The silicon concentrations in the control groups measured after 6h and 24h were below the LOD (<5-14 mg silicon/kg tissue depending the organ) in all sampled organs, except in the ovaries 6h after the start of the experiments, where a silicon concentration of 11 ± 5 mg/kg was measured (LOD = 11 mg/kg). In the gastrointestinal contents of the control animals, Si concentrations were high (> 500 mg/kg) due to the ingestion of standard feed and drinking water, both containing naturally occurring silica.

In treated animals, the target organs where most Si accumulated in both the 6h and 24h-groups, were the liver and the spleen (Fig. 3). In the 6h-group, most of the supplied dose of silicon was detected in the liver (64 ± 22%) while 1.5 ± 0.6% of the applied dose was found in the spleen. Similar results were found 24h after treatment: 54 ± 14% of the injected silicon was detected in the liver and 1.0 ± 0.7% in the spleen. Besides liver and spleen, low concentrations of silicon were detected in the bladder and lungs, and in the ovaries 6h after the start of the experiments (Fig. 3). In the latter case the average concentration (12 ± 7 mg/kg) did, however, not differ from the one in the control animals. The silicon concentrations were below the detection limit in pancreas, kidney, uterus, heart, muscle, brain and blood, and in the ovaries 24h after the start of the experiments.

In spleen, the silicon concentration decreased significantly (p = 0.035) from 130 ± 41 mg/kg after six hours to 65 ± 24 mg/kg after 24 hours. In liver, the silicon concentration tended to decrease between 6h and 24h but it was not significant. In other tissues, the silicon concentration was too low and the variability too high to determine any trend (Fig. 3).

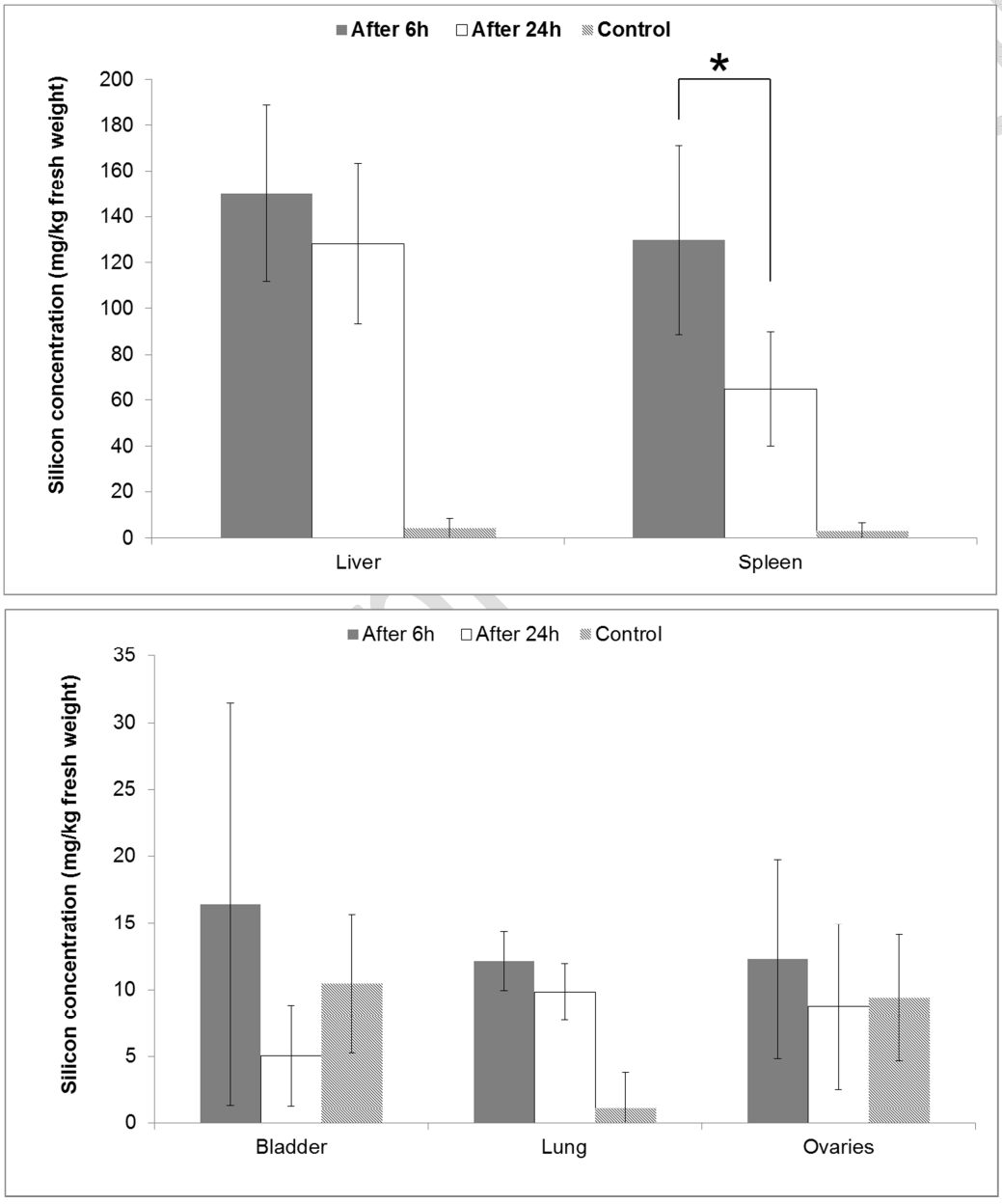

Fig. 3. Silicon concentration in tissues (mg/kg fresh weight), 6h (dark grey column) or 24h (white column) after intravenous administration of NM-200 (20 mg/kg bodyweight), and of control animals. Data are expressed as the mean ± standard deviation (n = 5). Note that the mean silicon concentrations in the tissues of the control animals and in the bladder and ovaries 24h after intravenous administration are all below their respective limit of detection. *P < 0.05 comparison between the 6h and 24h evaluation moments.

The total recovery of the applied dose of silicon in tissues and urine was 85 ± 14% after 24h and 72 ± 24% after six hours, except for one animal where only 11% of the applied dose was recovered. As there were some problems during the IV injection, this individual was not taken into account in the recovery calculations. The amount of silicon not recovered could be either in non-sampled remaining tissues or more likely in the gastro-intestinal tract content, where it cannot be distinguished from dietary silicon. The recoveries of the applied dose in tissues and urine are acceptable in comparison to other studies. In the NANOGENOTOX project for example, 58 ± 10% of the applied dose was recovered in the analyzed tissues [18].

3.4. Silicon excretion

To determine the silicon excretion after IV exposure, the silicon concentration was measured in urine, faeces and in the gastro-intestinal contents produced during 6 or 24 hours.

The silicon concentration in urine was significantly higher in treated (55 ± 19 mg/kg) versus control animals (30 ± 5 mg/kg) after 24 hours while there was no significant difference between the control and treated group after 6 hours (20 ± 7 vs 44 ± 18 mg/kg). Six hours after treatment with NM-200, 5 ± 2 % of

the supplied silicon dose was excreted via urine, while 24 hours after treatment, 32 ± 7 % of the supplied silicon dose was excreted by the urinary route.

Because the rats had free access to water and standard feed, the silicon concentration in the gastro-intestinal tract was high and variable both in control animals and treated rats (Fig. 4). As fecal excretion of silicon resulting from IV injection cannot be separated from the unabsorbed silicon fraction present in feed, the excretion rates cannot be calculated. There were, however, no significant differences in the Si concentrations in the gastrointestinal tract between the control and treated groups.

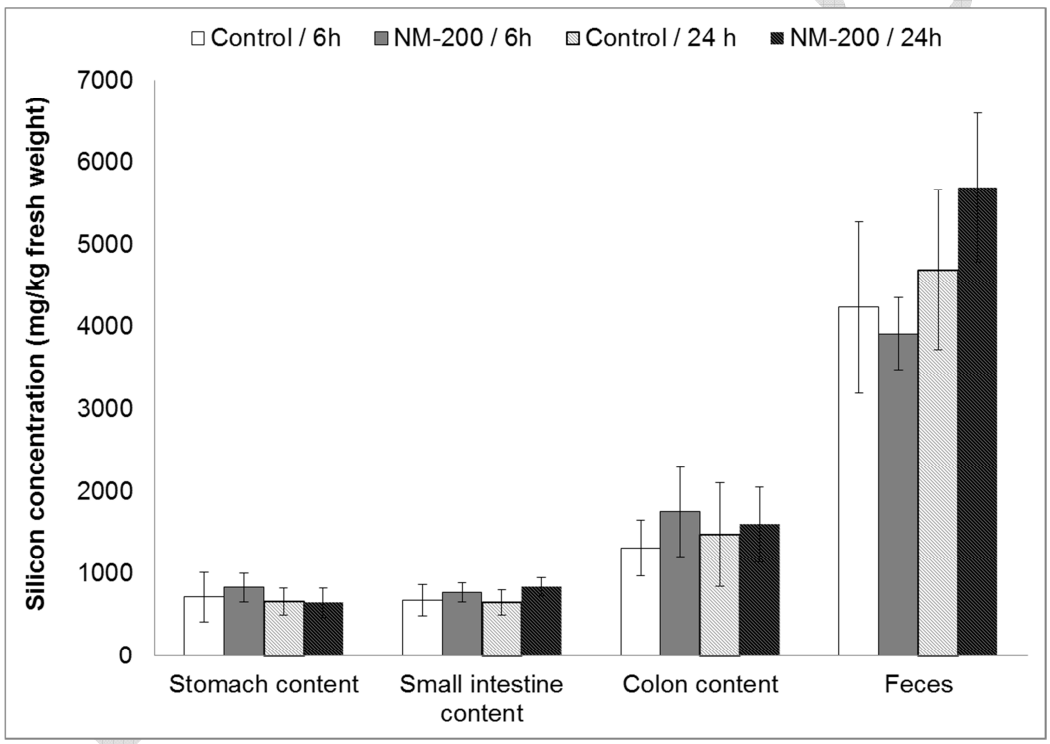

Fig. 4. Silicon concentration in the gastro-intestinal tract (mg/kg fresh weight), 6h or 24h after intravenous administration of NM-200 (20 mg/kg bodyweight) or PBS (Control). Data are expressed as the mean ± standard deviation (n = 5).

4. DISCUSSION

Animals had free access to drinking water and standard laboratory feed, both containing naturally occurring silica. This probably leads to a certain level of silicon in the animal tissues. As suggested by van der Zande et al. ([5], and references therein), silicon is likely present as sodium, calcium and magnesium silicates or as soluble hydrated silica $SiO_2.nH_2O$, which may contain small polysilicic acid particles in the size range of 1–5 nm. The silicon concentration in feed and water was not measured in the current study. As the control animals received the same diet, the comparison between the groups remains, however, valid.

When nanoparticles enter the body, a variety of serum proteins bind to their surface, which are recognized by the scavenger receptors on the macrophage cell surface and are quickly removed from circulation [11, 31]. Hence nanosilica is not detected in blood because it is rapidly cleared from the blood circulation [22, 32]. These macrophages are part of the reticulo-endothelial system and are especially numerous in the spleen (red pulp macrophage) and in in the liver (Kupfer cells) [11-12, 16, 22, 33-34], as shown by immunohistochemical results with CD68. This explains the high concentration of silicon in liver and spleen after injection with NM-200, especially as these organs are highly vascularized due to their involvement in blood filtration (spleen) and detoxification (liver). Previous studies also recorded liver and spleen as target organs both after single and repeated IV exposure to nanosilica [10-12, 15-18]. Twenty four hours after a single dose IV administration of NM-200 to female rats, we found highest silicon concentrations in liver, which corresponds to the results of the NANOGENOTOX project [18]. Six hours after IV administration silicon concentrations in spleen and in liver, however, were similar, but a significant decrease in the silicon concentration in spleen had taken place between 6 and 24 hours after injection. Within the NANOGENOTOX project, 24 hours after IV administration similar silicon

concentrations in liver and spleen of female rats were noted for NM-203, but not for NM-200 [18]. The authors concluded that there was a difference in particle biodistribution between both types of nanoparticles, with a higher presence of NM-203 in spleen compared to NM-200 [7, 18]. Based on the current observations it is suggested that both types of nanoparticles initially accumulate preferentially in the spleen and thus have a similar biodistribution, but NM-200 is faster cleared from the spleen than NM-203. This is also corroborated by blood silicon concentrations within the first 24 hours after IV administration, as in the 2 to 8 hour-period after administration of NM-200, silicon was present in blood in detectable concentrations that were larger than those of NM-203 [18]. Hence biodistribution between both types of SiO_2NP is probably similar in female rats, but biokinetics probably differ. NM-200 may be rapidly driven to the liver through the splenic vein and the hepatic portal vein, which also collects blood from the gastro-intestinal tract. Silicon in the liver is then excreted by the hepatobiliary route [11-12, 15, 21]. The clearance of the liver is slowed down by the reabsorption of a fraction of the SiO_2NP by the gastro-intestinal tract [5, 35].

The main route of NM-200 excretion in the first 24 hours was the urinary route, which is in accordance with previous studies [12, 19, 22]. Biliary and fecal excretion of NM-200 could not be demonstrated in the current study. This might be due to the high Si background in the GI tract resulting from SiO_2 in the feed of the animals, but also due to the slower process of SiO_2 excretion through the biliary route. Renal excretion of SiO_2 NP peaks a few hours after IV injection, before decreasing rapidly in the following hours [12, 19]. Fecal excretion of SiO_2NP through the biliary route peaks, on the contrary, after several hours to several days before slowly decreasing [12, 19, 22]. According to Huang et al. [12] the possible reason for this lag is the difference in speed between the excretion processes involved. Excretion of silica through feces may be performed by hepatic processing and biliary excretion after liver uptake, which is relatively

slow. In contrast, excretion of silica in urine by the mechanism of tubular secretion, directly from the plasma into the tubular fluid, is a much faster process than hepatic excretion [19].

Further research is needed with lower exposure doses to predict kinetics and toxicity of silica nanoparticles depending on their physicochemical characteristics. Silica from food has been estimated to be ingested by humans at a rate of 9.4 mg/kg_{bw}/day, of which 1.8 mg/kg_{bw}/day may be in the nanoscale range [2]. Only a fraction of this nanosilica is absorbed by the gastro-intestinal tract. Oral and IV exposure at such doses, although analytically challenging, could provide interesting information for a realistic hazard assessment. Furthermore, IV exposure to different particle types and at more time intervals could help to clarify whether kinetics and biodistribution are the same or could differ depending on silica NM (e.g. NM-200 vs NM-203).

5. CONCLUSION

After an intravenous exposure of female rats to NM-200, the main target organs for SiO_2NP accumulation were the liver and the spleen, 6h as well as 24 hours after treatment. Six hours after injection, the silicon concentrations in both organs were similar, but in spleen the silicon concentration significantly decreased with time. NM-200 in the spleen may be rapidly driven to the liver via the hepatic portal vein while clearance of the liver takes more time due to hepatic processing and biliary excretion, and due to the reabsorption of a fraction of the SiO_2NP from the gastro-intestinal tract. The silicon concentration in the other organs was below the LOQ. Within the first 24 hours NM-200 was mainly excreted through urine. The short-time exposure to NM-200 at a dose of 20 mg/kg_{bw} did not show histopathological toxicity.

Based on a comparison of our results with those from the NANOGENOTOX project, the similarity in the biodistribution of two different SiO_2 NM, namely NM-200 and NM-203, in female rats became evident, while biokinetics between both types of SiO_2NP was suggested to differ. Further studies are needed to determine which characteristics can have an impact on the toxicokinetic parameters in order to predict or infer kinetics and toxicity of silica nanomaterials.

ACKNOWLEDGEMENTS

The authors wish to thank Mathias Truyens and Fred Stockmans for taking care of the experimental animals and their assistance during autopsy, Jorina Gheys for preparing the ethical dossier and her help in the *in vivo* experimental setup and Lotte Delfosse for the silicon analyses of the biological samples. The authors of this article also wish to thank Riet Geeroms, Gaël Landuyt and Mathieu Pakula for their technical assistance.

DECLARATION OF INTEREST

This research was commissioned and financed by the Belgian Federal Public Service of Health, Food Chain Safety and Environment [Project RT 10/05 NANORISK]. The funding authority was neither involved in the study design, data analysis and interpretation, nor in the preparation of this manuscript.

REFERENCES:

[1] Commission Regulation of the European Union, Commission Regulation (EU) No 1130/2011, Amending Annex III to Regulation (EC) No 1333/2008 of the European Parliament and of the Council on food additives by establishing a Union list of food additives approved for use in food additives, food enzymes, food flavourings and nutrients, Official Journal of the European Union L295 (2011), pp. 178–204.

[2] S. Dekkers, P. Krystek, R.J.B.Peters, D.P.K. Lankveld, B.G.H. Bokkers, P.H. Van Houven-Arentzen, H. Bouwmeester, A.G. Oomen, Presence and risks of nanosilica in food products, Nanotoxicology, 5 (2011), pp. 393-405.

[3] P.J. De Temmerman, E. Van Doren, E. Verleyssen, Y. Van der Stede, M.A.D. Francisco, J. Mast, Quantitative characterization of agglomerates and aggregates of pyrogenic and precipitated amorphous silica nanomaterials by transmission electron microscopy, J. Nanobiotechnology, 10 (2012), pp. 24.

[4] S.J. So, I.S. Jang, C.S. Han, Effect of micro/nano silica particle feeding for mice, J. Nanosci. Nanotechnol., 8 (2008), pp. 5367–5371.

[5] M. van der Zande, R.J. Vandebriel, M.J. Groot, E. Kramer, Z.E. Herrera Rivera, K. Rasmussen, J.S. Ossenkoppele, P. Tromp, E.R. Gremmer, R.J. Peters, P.J. Hendriksen, H.J. Marvin, R.L. Hoogenboom, A.A. Peijnenburg, H. Bouwmeester, Sub-chronic toxicity study in rats orally exposed to nanostructured silica, Fibre Toxicol., 11 (2014), pp. 8-27 .

[6] J.A. Lee, M.K. Kim, J.H. Song, M.R. Jo, J. Yu, K.M. Kim, Y.K. Rok, J.M. Oh, S.J. Choi, Biokinetics of food additive silica nanoparticles and their interactions with food components, Colloid. Surface. B., 150 (2017), pp. 384-392.

[7] P.C.E. van Kesteren, F. Cubadda, H. Bouwmeester, J.C.H. van Eijkeren, S. Dekkers, W.H. De Jong, A.G. Oomen, Novel insights into the risk assessment of the nanomaterial synthetic amorphous silica, additive E551, in food; Nanotoxicology, 9 (2015), pp. 442-452.

[8] S. Bellmann, D. Carlander, A. Fasano, D. Momcilovic, J.A. Scimeca, W.J. Waldman, L. Gombau, L. Tsytsikova, R. Canady, D.I.A. Pereira, D.E. Lefebvre, Mammalian gastrointestinal tract parameters modulating the integrity, surface properties, and absorption of food-relevant nanomaterials, WIREs Nanomed. Nanobiotechnol., 7 (2015), pp. 609-622.

[9] K. Sakai-Kato, M. Hidaka, T. Kawanishi, H. Okuda, Physicochemical properties and in vitro intestinal permeability properties and intestinal cell toxicity of silica particles, performed in simulated gastrointestinal fluids, BBA-Gen. Subjects, 1840 (2014), pp. 1171-1180.

[10] Q. He, Z. Zhang, F. Gao, Y. Li, J. Shi, In vivo biodistribution and urinary excretion of mesoporous silica nanoparticles: effects of particle size and PEGylation, Small, 7 (2011), pp. 271-280.

[11] R. Kumar, I. Roy, T.Y. Ohulchanskky, L.A. Vathy, E.J. Bergey, M. Sajjad, P.N. Prasad, *In vivo* biodistribution and clearance studies using multimodal organically modified silica nanoparticles, ACS Nano, 4 (2010), pp. 699-708.

[12] X. Huang, L. Li, T. Liu, N. Hao, H. Liu, D. Chen, F. Tang, The shape effect of mesoporous silica nanoparticles on biodistribution, clearance, and biocompatibility in vivo, ACS Nano, 5 (2011), pp. 5390-5399.

[13] H. Nishimori, M. Kondoh, K. Isoda, S. Tsunoda, Y. Tsutsumi, K. Yagi, Histological analysis of 70-nm silica particles-induced chronic toxicity in mice, Eur. J. Pharm. Biopharm., 72 (2009), pp. 626-9.

[14] Y. Guichard, M.A. Maire, S. Sébillaud, C. Fontana, C. Langlais, J.C. Micillino, C. Darne, J. Roszak, M. Stępnik, V. Fressard, S. Binet, L. Gaté, Genotoxicity of synthetic amorphous silica nanoparticles in

rats following short-term exposure, part 2 : intratracheal instillation and intravenous injection, Environ. Mol. Mutagen., 56 (2015), pp. 228-244.

[15] C. Fu, T. Liu, L. Li, H. Liu, D. Chen, F. Tang, The absorption, distribution, excretion and toxicity of mesoporous silica nanoparticles in mice following different exposure routes, Biomaterials, 34 (2013), pp. 2565-75.

[16] T. Liu, L. Li, X. Teng, X. Huang, H. Liu, D. Chen, J. Ren, J. He, F. Tang, Single and repeated dose toxicity of mesoporous hollow silica nanoparticles in intravenously exposed mice, Biomaterials, 32 (2011), pp. 1657-68.

[17] S. Zhuravskii, G. Yukina, O. Kulikova, A. Panevin, V. Tomson, D. Korolev, M. Galagudza, Mast cell accumulation precedes tissue fibrosis induced by intravenously administered amorphous silica nanoparticles, Toxicol. Mech. Method., 26 (2016), pp. 260-269.

[18] W.H. De Jong, N.R. Jacobsen, H. Wallin, A. Oomen, E. Brandon, P. Krystek, M. Apostolova, I. Karadjova, F. Cubadda, F. Aureli, F. Maranghi, V. Dive, F. Taran, B. Czarny, NANOGENOTOX, Deliverable 7: Identification of target organs and biodistribution including ADME parameters. Final Report, Bilthoven, The Netherlands: National Institute for Public Health and Environment (RIVM), (2013). Available at: http://www.nanogenotox.eu/files/PDF/DELIVRABLES2/deliverable7__biodistribution.pdf (Accessed 01-07-2016).

[19] M.A. Malfatti, H.A. Palko, E.A. Kuhn, K.W. Turteltaub, Determining the pharmacokinetics and long-term biodistribution of SiO2 nanoparticles in vivo using accelerator mass spectrometry, Nano Lett., 12 (2012), pp. 5532-8.

[20] G. Xie, J.Sun, G. Zhong, L. Shi, D. Zhang, Biodistribution and toxicity of intravenously administered silica nanoparticles in mice, Arch. Toxicol., 84 (2010), pp. 183-190.

[21] M. Cho, W.S. Cho, M. Choi, S.J. Kim, B.S. Han, S.H. Kim, H.O. Kim, Y.Y. Sheen, J. Jeong, The impact of size on tissue distribution and elimination by single intravenous injection of silica nanoparticles, Toxicol. Lett., 189 (2009), pp. 177-83.

[22] T. Yu, D. Hubbard, A. Ray, H. Ghandehari, In vivo biodistribution and pharmacokinetics of silica nanoparticles as a function of geometry, porosity and surface characteristics, J. Controlled Release, 163 (2012), pp. 46-54.

[23] P. Decuzzi, B. Godin, T. Tanaka, S.Y. Lee, C. Chiappini, X. Liu, M. Ferrari, Size and shape effects in the biodistribution of intravascularly injected particles, J. Controlled Release, 141 (2010), pp. 320-327.

[24] OECD, Guidance manual for the testing of manufactured nanomaterials: OECD's sponsorship programme; first revision. OECD Environment, Health and Safety Publications Series on the Safety of Manufactured Nanomaterials ENV-JM-MONO(2009)20-REV-ENG. Paris, France, (2010) .

[25] JRC-IHCP, Synthetic amorphous silicon dioxide (NM-200, NM-201, NM-202, NM-203, NM-204): characterisation and physico-chemical properties. Ispra, Italy: Joint Research Centre, Institute for Health and Consumer Protection, (2013).

[26] K. Jensen, Y. Kembouche, E. Christiansen, N. Jacobsen, H. Wallin, The generic NANOGENOTOX dispersion protocol. *In*: K. Jensen, N. Thieret (Eds.), Standard Operation Procedures (SOP) and background documentation: Final Protocol for producing suitable manufactured nanomaterial exposure media, (2011).

[27] P.J. De Temmerman, E. Verleysen, J. Lammertyn, J. Mast Size measurement uncertainties of near-monodisperse, near-spherical nanoparticles using transmission electron microscopy and particle-tracking analysis, J. Nanopart. Res., 16 (2014), pp. 1-17.

[28] OECD, Test No 417: Toxicokinetics, OECD Guidelines for the Testing of Chemicals, Section 4: Health effects, (2010). Available at:

http://www.oecd-ilibrary.org/environment/test-no-417-toxicokinetics_9789264070882-en. (Accessed 12-01-2012).

[29] E.F. McInnes, Background lesions in laboratory animals: A color atlas. Chapter 2: Wistar and Sprague-Dawley rats. Saunders Elsevier, Edinburgh. pp. 20-22, (2012).

[30] P. Klemens, K.G. Heumann, Development of an ICP-HRIDMS method for accurate determination of traces of silicon in biological and clinical samples, Fresenius J. Anal. Chem., 371 (2001), pp. 758-63.

[31] P. Opanasopit, M. Nishikawa, M. Hashida, Factors affecting drug and gene delivery: effects of interaction with blood components, Crit. Rev. Ther. Drug Carrier Syst., 19 (2002), pp. 191–233.

[32] L.M. Bimbo, M. Sarparanta, H.A. Santos, A.J. Airaksinen, E. Mäkilä, T. Laaksonen, L. Peltonen, V.P. Lehto, J. Hirvonen, J. Salonen, Biocompatibility of thermally hydrocarbonized porous silicon nanoparticles and their biodistribution in rats, ACS Nano, 4 (2010), pp. 3023-3032.

[33] H. Nishimori, M. Kondoh, K. Isoda, S., Tsunoda, Y. Tsutsumi, K. Yagi, Silica nanoparticles as hepatotoxicants, Eur. J. Pharm. Biopharm., 7 (2009), pp. 496-501.

[34] Y. Yu, Y. Li W. Wang, M. Jin, Z. Du, Y. Li, J. Duan, Y. Yu, Z. Sun, Acute toxicity of amorphous silica nanoparticles in intravenously exposed ICR mice, PLoS One, 8(4) (2013), pp. e61346.

[35] T. Liu, H. Liu, C. Fu, L. Li, D. Chen, Y. Zhang, F. Tang, Smaller silica nanorattles reabsorbed by intestinal aggravate multiple organs damage, J. Nanosci. Nanotechnol., 13 (2013), pp. 6506-16.